Neutron powder diffraction study of the low-temperature phases of KNO_2

Neutron powder diffraction study of the low-temperature phases of KNO$_2$

N Onoda-Yamamuro†¶, H Honda†+, R Ikeda†*, O Yamamuro‡,
T Matsuo‡, K Oikawa§, T Kamiyama§ and F Izumi‖

† Department of Chemistry, University of Tsukuba, Tennodai, Tsukuba, Ibaraki 305, Japan
‡ Department of Chemistry and Microcalorimetry Research Centre, Graduate School of Science, Osaka University, Machikaneyama-cho 1-1, Toyonaka, Osaka 560, Japan
§ Institute of Materials Science, University of Tsukuba, Tennodai, Tsukuba, Ibaraki 305, Japan
‖ National Institute for Research in Inorganic Materials, 1-1 Namiki, Tsukuba, Ibaraki 305, Japan

Abstract. We made neutron powder diffraction measurements for phase III (at 4, 120, 180, 220, and 250 K) and phase II (at 280 K) of KNO$_2$. The structure of phase III was determined by the Rietveld method using the data obtained at 4 K; the initial structure parameters were obtained by a systematic trial-and-error method. Phase III is monoclinic (space group: $P2_1/c$) with $a = 4.4010(2)$ Å, $b = 9.5967(3)$ Å, $c = 6.9817(2)$ Å, $\beta = 108.274(3)°$, and $Z = 4$. Both K$^+$ and NO$_2^-$ ions are located at general positions, and the orientations of the NO$_2^-$ ions are completely ordered. The structures of phase III at the higher temperatures were also examined on the basis of the structure at 4 K. The atomic displacement parameters of the NO$_2^-$ ions increased anomalously with increasing temperature, indicating gradual but remarkable development of the orientational disorder of NO$_2^-$ ions. The structure of phase II was determined to be rhombo-hedral (space group: $R\bar{3}m$) with $a = 5.02790(4)$ Å, $c = 10.05587(8)$ Å, and $Z = 3$. The orientations of the NO$_2^-$ ions were highly disordered about the $\bar{3}$ axis.

1. Introduction

Potassium nitrite, KNO$_2$, forms three crystalline phases, I, II, and III, depending on the temperature [1]. The structure of each phase has been studied by means of single-crystal x-ray diffraction [2]. Phase I ($T > 315$ K) has a NaCl-type cubic structure in which the orientations of the NO$_2^-$ ions are spherically disordered. Because of the disorder, the crystal deforms easily under a weak stress, and thus is classified as a plastic crystal. The structure of phase II (264 K $< T <$ 315 K) is rhombohedral (space group: $R\bar{3}m$), and the orientations of the NO$_2^-$ ions are still disordered about a $\bar{3}$ axis. For phase III ($T < 264$ K), a monoclinic cell with space group $P2_1/c$ has been reported [2]. The orientations of the NO$_2^-$ ions have not been determined yet, but they were assumed to be ordered because of the low symmetry of the crystal structure. No further structural study has been carried out for phase III.

¶ Present address: Department of Chemical Technology, Kurashiki University of Science and the Arts, 2640 Nishinoura, Tsurajima-cho, Kurashiki-shi, Okayama 712, Japan.
+ Present address: Faculty of Science, Yokohama City University, Seto, Kanazawa-ku, Yokohama 236, Japan.
* Author to whom any correspondence should be addressed; e-mail: ikeda@staff.chem.tsukuba.ac.jp; fax: +81-298-53-6503; telephone: +81-298-53-4250.

Phase III, which is the chief concern of this study, is unusual in that its heat capacity exceeds the normal vibrational value at temperatures as low as 100 K, and increases further with increasing temperature toward the III–II transition [1]. The excess entropy due to this anomaly is larger than the first-order component of the III–II transition entropy as shown in figure 1. Such an anomaly has never been observed in molecular plastic crystals, and so could be a characteristic feature of ionic plastic crystals. The heat capacity anomaly suggests that the orientations of the NO_2^- ions become disordered gradually with increasing temperature over an extremely wide temperature range in phase III. Our ^{15}N and ^{39}K NMR [3] and dielectric [4] studies also supported the orientational disorder of the NO_2^- ions; i.e., a minimum of the spin–lattice relaxation time T_1 appeared at about 160 K in both ^{15}N and ^{39}K data. Dielectric dispersion occurred in the temperature range 50–120 K for the frequency range $20–10^6$ Hz. We proposed that these effects arise from the 180°-flipping motion of the NO_2^- ions in phase III.
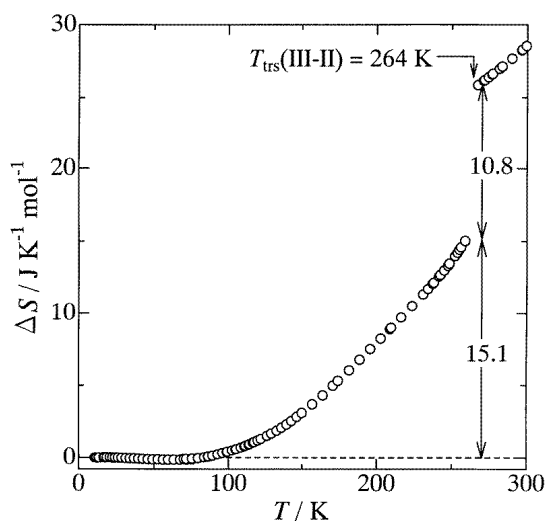

Figure 1. The temperature dependence of the excess entropy of KNO_2 calculated from heat capacity data available in the literature [1].

As described above, there is disagreement as to the orientations of the NO_2^- ions in phase III; i.e. structural study [2] suggests orientational ordering of the NO_2^- ions while the calorimetric [1], NMR [3], and dielectric [4] studies favour orientational disorder. The main purpose of the present study is to examine the orientational order/disorder of the NO_2^- ions in phase III by neutron diffraction. We have collected neutron powder diffraction data on phase III at several temperatures to investigate the temperature dependence of the structure as well. It is an additional aim of the present work to investigate the orientational disorder of NO_2^- ions in phase II. This phase has been examined by means of single-crystal x-ray diffraction, and two structural models have been proposed for the orientations of NO_2^- ions [2]. One of them was regarded as more satisfactory on the basis of the bond lengths. Neutron diffraction is useful for determination of the positions of the disordered N and O atoms which can hardly be distinguished using x-ray diffraction. The coherent neutron scattering lengths of N and O atoms are different enough (9.36 fm and 5.803 fm, respectively) for them to be differentiated by this method.

2. Experimental procedure

As a commercial KNO$_2$ sample contained $\simeq 0.5\%$ of Na$^+$ ions and $\simeq 3\%$ of NO$_3^-$ ions, the sample of KNO$_2$ used in this study was prepared from NaNO$_2$ (Wako Pure Chemical Industries, Limited) using a cation-exchange method (Diaion SK-1 resin, Mitsubishi Kasei Corporation). The product was further purified by recrystallization from water. The purity of the sample was checked by ICP emission spectroscopy (Ash ICAP-757V, Nippon Jarrell) and ion chromatography (IC 100, Yokogawa) at the Chemical Analysis Centre, University of Tsukuba. The number fractions of the ions were as follows: K$^+$: 49.95%; Na$^+$: 0.05%; NO$_2^-$: 50.0%; NO$_3^-$: 0.0%.

The neutron powder diffraction data on KNO$_2$ were collected on the time-of-flight (TOF) diffractometer VEGA [5] installed at the Neutron Science Laboratory (KENS) of the High Energy Accelerator Research Organization (KEK). The purified sample ($\simeq 3.5$ g) was contained in a vacuum-tight cylindrical can made of vanadium (5 mm in diameter and 50 mm in height) under a helium atmosphere. The TOF range of 4.5–42 ms, corresponding to the d-spacing range of 0.5–4.3 Å, was covered in these measurements. The resolution of the diffraction data ($\Delta d/d$) was about 0.2%. The diffraction data on phase III were measured at 4, 120, 180, 220, and 250 K, and those on phase II at 280 K.

Table 1. Refined structural parameters for KNO$_2$ at 4 K. Anisotropic temperature factor: $T = \exp[-2\pi^2(h^2 a^{*2} U_{11} + k^2 b^{*2} U_{22} + l^2 c^{*2} U_{33} + 2hka^*b^* U_{12} + 2hla^*c^* U_{13} + 2klb^*c^* U_{23})]$. Monoclinic: space group $P2_1/c$ (No 14). Lattice constants: $a = 4.4010(2)$ Å, $b = 9.5967(3)$ Å, $c = 6.9817(2)$ Å, $b = 108.274(3)°$, $Z = 4$. $R_B = 1.44\%$, $R_{wp} = 4.34\%$, $R_e = 3.83\%$, and $S = 1.13$ for 3348 profile points and 107 variables.

	x	y	z	B (Å^2)
K	0.4105(8)	0.1407(3)	0.2101(5)	0.13(7)
N	−0.0732(4)	0.4107(2)	0.1839(2)	—
O(1)	0.2034(5)	0.4127(3)	0.3067(3)	—
O(2)	−0.1615(7)	0.2999(2)	0.0865(3)	—

	U_{11} (Å^2)	U_{22} (Å^2)	U_{33} (Å^2)	U_{12} (Å^2)	U_{13} (Å^2)	U_{23} (Å^2)	B_{eq} (Å^2)
N	0.0057(8)	0.0022(7)	0.0060(8)	0.0011(8)	−0.0002(7)	−0.0012(7)	0.40
O(1)	0.001(1)	0.005(1)	0.006(1)	0.0002(14)	−0.002(1)	−0.0008(11)	0.37
O(2)	0.004(1)	0.006(1)	0.003(1)	0.0004(11)	−0.003(1)	−0.0004(10)	0.39

3. Results and discussion

3.1. The structure of phase III

The unit-cell dimensions of phase III were determined by using 48 distinct reflections in a low-Q region ($1.2 < d/\text{Å} < 4.2$). The auto-indexing program DICVOL-91 [6] gave a monoclinic cell ($a = 4.401(2)$ Å, $b = 9.596(2)$ Å, $c = 6.981(2)$ Å, $\beta = 108.28(4)°$, and $Z = 4$) with figures of merit $M(48) = 9.4$ [7] and $F(48) = 16.0$ [8]. From the systematic absence of reflections ($h0l$: $h + l \neq 2n$; $0k0$: $k \neq 2n$), the space group was determined to be $P2_1/c$. This space group was confirmed by Pawley refinement [9] using the program CAILS [10]. The space group thus determined was the same as suggested by the previous x-ray diffraction study [2]. In this structure, one molecule forms the asymmetric unit, which indicates that the NO$_2^-$ ions are located at general positions and that all of the NO$_2^-$ ions

Table 2. Selected intra- and inter-ionic bond lengths (Å) and angles (deg). (The symmetry codes are: (i) $x, 1/2 - y, -1/2 + z$; (ii) $1 - x, -1/2 + y, 1/2 - z$; (iii) $1 + x, y, z$; and (iv) $1 + x, 1/2 - y, 1/2 + z$.)

(a) Intra-ionic distances	
N–O(1)	1.250(2)
N–O(2)	1.256(2)
O(1)–N–O(2)	116.9(2)

(b) Shortest inter-ionic K$\cdots$O distances	
K$\cdots$O(1$^{\text{i}}$)	2.723(4)
K$\cdots$O(1$^{\text{ii}}$)	2.796(4)
K$\cdots$O(1)	2.912(4)
K$\cdots$O(2$^{\text{iii}}$)	2.766(4)
K$\cdots$O(2$^{\text{iv}}$)	2.771(4)
K$\cdots$O(2)	2.838(4)

are crystallographically equivalent.

We searched for a starting model for the Rietveld refinement by a trial-and-error method. The program used was RIETAN-96T [11]. A number of trial models were constructed by changing the positions and orientations of the K^+ and the NO_2^- ions on the basis of the known structures of several NO_2 and NO_3 compounds. For each model, a quick Rietveld refinement was performed using a limited number of parameters. A slack-constraint technique was utilized in this stage: the N–O bond length and O–N–O angle were constrained to be within 1.24 ± 0.2 Å and $115.0 \pm 2.5°$, respectively. The expected values of the bond lengths and the angles were taken from the corresponding data on $NaNO_2$ [12]. A model derived from the structure of NH_2NO_2 [13] gave a satisfactorily small S-value ($=R_{wp}/R_e$) for a starting structure. The next stage of the refinement was performed without any constraint on the structural parameters. Anisotropic atomic displacement parameters were assigned to N and O atoms in this stage. A new technique, called partial profile relaxation [11], was used in the final stage of the refinement and gave an excellent S-value of 1.13 (compare, e.g., 1.61 obtained by a previous method). The 107 variable parameters (15 background parameters, 1 extinction parameter, 1 scale factor, 13 profile parameters, 42 additional profile parameters for the partial profile relaxation method, 4 lattice constants, 12 atomic coordinates, 19 isotropic and anisotropic atomic displacement parameters) were refined using 3348 intensity data in the TOF range between 5.5 and 41 ms ($d = 0.55$–4.1 Å). The final structural parameters are summarized in table 1. Table 2 lists the intra-ionic N–O and inter-ionic K$\cdots$O bond lengths and the O–N–O bond angle calculated from the refined fractional coordinates. All of the intra-ionic parameters determined are reasonable compared with the corresponding values for $NaNO_2$ (see above). The final results of the profile fitting are illustrated in figure 2.

The structure of KNO_2 at 4 K is illustrated in figure 3(a), and its projection along the c-axis is shown in figure 3(b). The orientations of the NO_2^- ions are completely ordered. As shown by the dashed lines in figure 3(b), each K^+ ion is surrounded by six O atoms of the NO_2^- ions, with K$\cdots$O distances of 2.74–2.90 Å.

The present structure is different from the structure of the ordered phase (phase II) of KNO_3 [13], though their high-temperature (orientationally disordered) phases are identical, as detailed later. Phase II of KNO_3 has an orthorhombic structure (space group: *Pnma*),
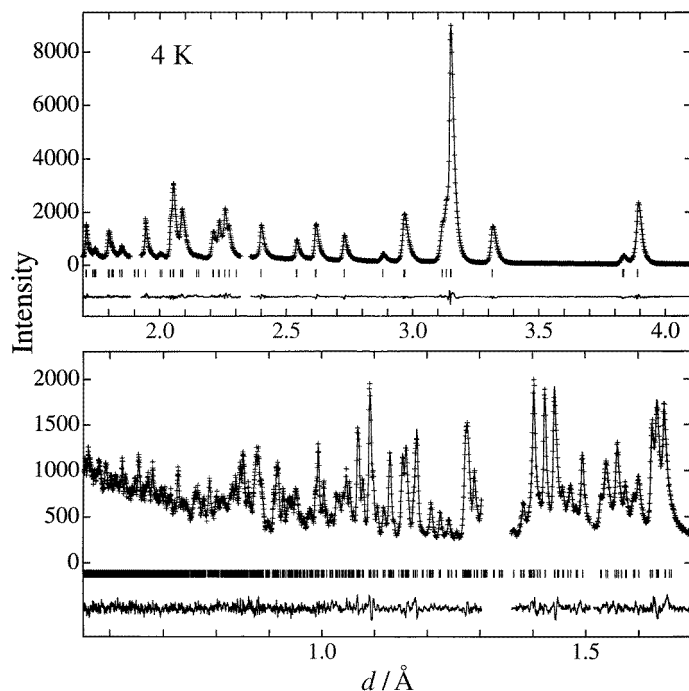
Figure 2. Observed (plus marks) and calculated (solid line) powder diffraction patterns of phase III at 4 K. The calculated peak positions are given by the short vertical bars, and the differences between the observed and calculated intensities are shown below them. The Bragg reflections from the sample environment, which was known from the empty run, were excluded from the refinement.
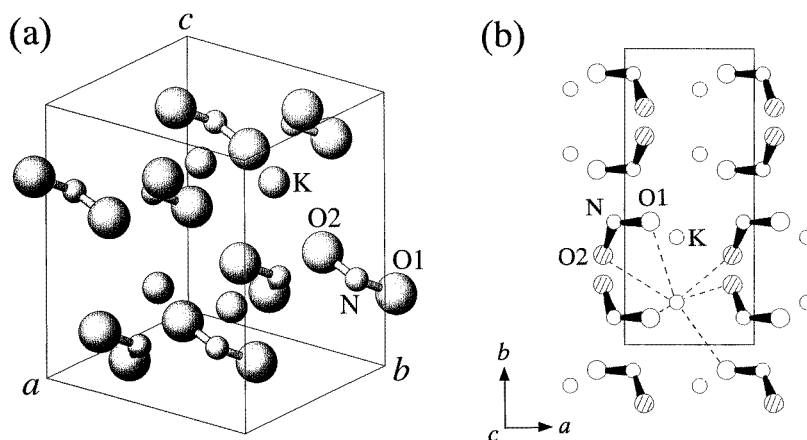

Figure 3. (a) A schematic illustration of phase III at 4 K. (b) A schematic view of the structure of phase III projected along the c-axis. The oxygen coordination around the K^+ ion is indicated by dashed lines (see table 2).

in which the K^+ ion, the N atom and one of the O atoms in the NO_3^- ion are located on a mirror plane [14]. The K^+ ion in phase II is surrounded by nine O atoms at K–O distances
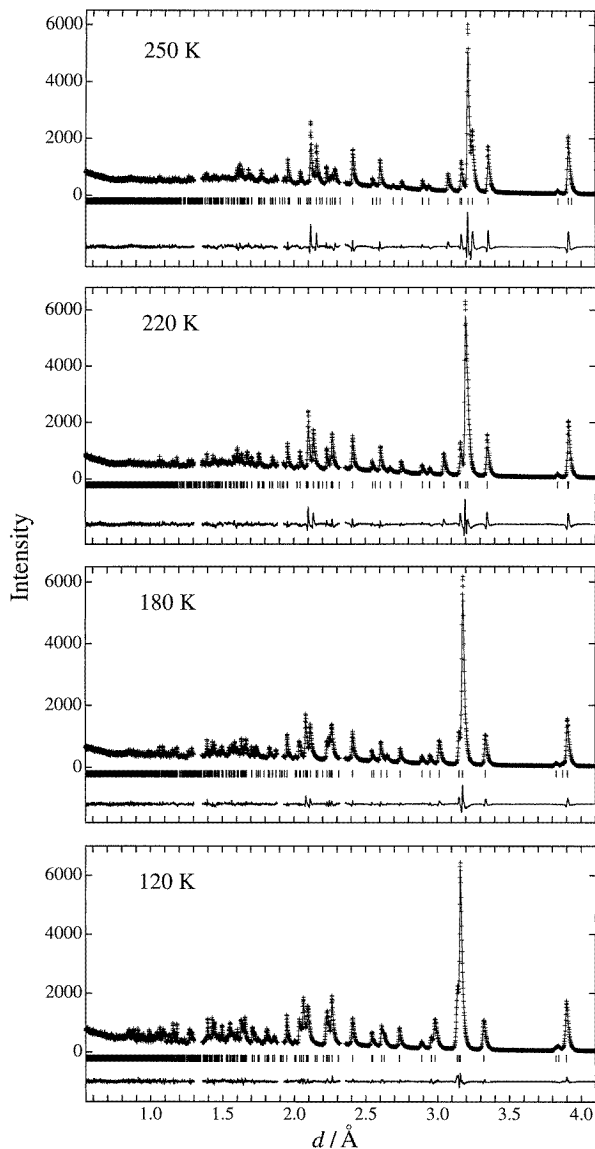
Figure 4. Observed (plus signs) and calculated (solid line) powder diffraction patterns of phase III at 120, 180, 220, and 250 K.

between 2.83 and 2.93 Å. Such a structural difference between KNO_2 and KNO_3 may be associated with the fact that the temperature at which the transition to the rhombohedral phase of KNO_2 (264 K) occurs is much lower than that for KNO_3 (401 K) [15].

In a series of monovalent nitrite crystals, the structure of $NaNO_2$ is ordered in the low-temperature phase and does not form a plastic phase. The structure of $NaNO_2$, which is orthorhombic, is quite different from the structure of KNO_2 phase III. On the other hand, $RbNO_2$, $CsNO_2$, and $TlNO_2$ form plastic phases as does KNO_2 [16–21]. However, the ordered structures of these nitrites have not been determined yet. It is most probable that

CsNO$_2$ and TlNO$_2$ do not form any ordered structures, because NO$_2^-$ ions are statically disordered at low temperatures in immobile glassy states [17]. The successful structure determination of KNO$_2$ phase III presented here may be significant as a unique case where the ordered structure into which an ionic plastically crystalline phase eventually transforms has been solved.

3.2. Orientational disorder of the NO$_2^-$ ions in phase III

The diffraction patterns of phase III at the higher temperatures (120, 180, 220, and 250 K) are shown by plus signs in figure 4. The peak positions and intensities change remarkably with increasing temperature. The significant decrease in intensities in a lower-d-spacing region suggests that the orientational disorder of the NO$_2^-$ ions develops with increasing temperature. These data were analysed by the Rietveld method using the structure at 4 K as the initial model for the refinements. The profile parameters were fixed throughout the refinement to reduce the number of variable parameters. Isotropic atomic displacement parameters were used for the final model because no significant improvement of the S-value was achieved by using anisotropic ones. The diffraction intensities calculated from the final refinement are shown by the solid line in figure 4. The final S-values for each of the refinements were as follows: 1.12 (120 K), 1.30 (180 K), 1.81 (220 K), 2.08 (250 K).
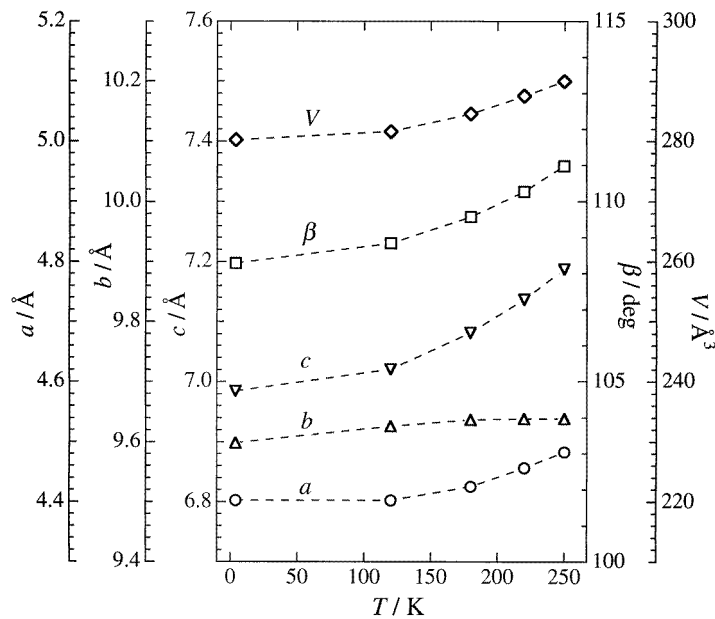

Figure 5. The temperature dependence of the lattice parameters (a, b, c, β) and volume (V) of the monoclinic cell of phase III.

Figure 5 shows the temperature dependence of the lattice parameters (a, b, c, β) and volume (V) of the monoclinic unit cell. It is of interest that b is not sensitive to temperature while a and c increase remarkably with increasing temperature. The isotropic atomic displacement parameter, B, is plotted as a function of temperature for each atom in figure 6. The parameters for phase II, which are determined in the next section, are included to demonstrate the effect of the III–II transition. $B(\text{K}^+)$ increases normally as a linear function
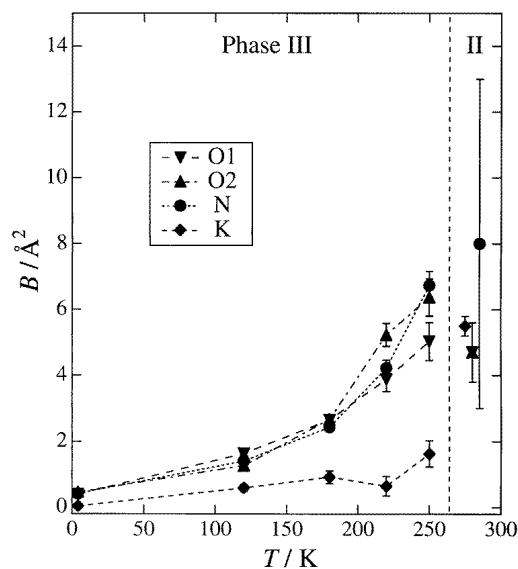
Figure 6. The temperature dependence of the atomic displacement parameters, *B*, for phases II and III. The data at 280 K are plotted with horizontal shifts of ±5 K to avoid overlapping.

of temperature while the *B*-values of the N, O1, and O2 atoms in the NO_2^- ion increase steeply as the temperature increases toward the III–II transition temperature. It is noteworthy that the temperature dependence of the *B*-values of N, O1, and O2 is similar to that of the excess entropy shown in figure 1, especially for the temperature at which the anomaly begins to be significant ($\simeq$100 K). The present results clearly indicate that the orientations of the NO_2^- ions become disordered gradually with increasing temperature, and the orientational disordering progresses more rapidly as the III–II transition temperature is approached.

At the III–II phase transition, no discontinuous change of the *B*-values of the N and O atoms was observed, in contrast with a discontinuous change of *B* for the K atom. In phase II, the NO_2^- ions undergo sixfold orientational disordering, as is described in the next section. Therefore, the present result indicates that the orientational disorder of the NO_2^- ions at higher temperatures of phase III is excited as much as in phase II.

At higher temperatures, the refinement results became less satisfactory with larger *S*-values, and the bond lengths, *l*, and angles, θ, for the NO_2^- ions deviate more from the ideal values; e.g., *l*(N–O1) = 1.14(1) Å, *l*(N–O2) = 1.03(1) Å, and θ(O1–N–O2) = 133(1)° at 250 K, compared with the ionic geometry of phase III given in table 2. This must be caused by the highly disordered orientation of the NO_2^- ions, which cannot be represented by the displacement parameters.

To make a further investigation of the orientational disorder of NO_2^- ions, we carried out a difference Fourier analysis. Figure 7 shows the difference Fourier contour maps of the section containing N, O1, and O2 atoms. The maximum density position of the N and two O atoms are connected by the solid straight lines. It is clearly shown that the density difference develops with increasing temperature. This means that some orientations other than the stable orientation determined at 4 K are excited at higher temperatures in phase III.

Detailed disorder models, such as those mixing two or more orientations of the NO_2^- ions with different probabilities, should improve the fitting for the data at higher temperatures if one can find appropriate initial models for the Rietveld refinement. In fact, refinements
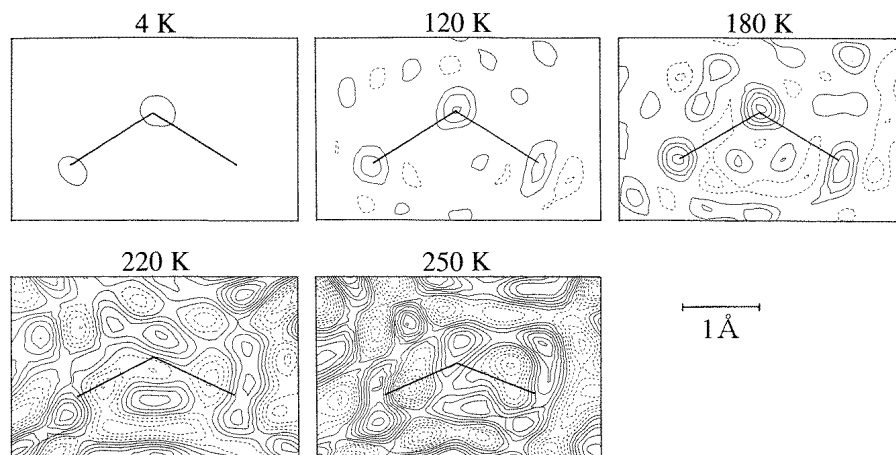
Figure 7. Difference Fourier contour maps for the section containing N, O1, and O2 atoms.

Table 3. Refined structural parameters for KNO$_2$ at 280 K. Rhombohedral: space group $R\bar{3}m$ (No 166). Lattice constants: $a = 5.027\,90(4)$ Å, $c = 10.055\,87(8)$ Å, $Z = 3$. $R_B = 5.42\%$, $R_{wp} = 3.88\%$, $R_e = 4.25\%$, and $S = 0.913$ for 3805 profile points and 44 variables.

	x	y	z	B (Å^2)
K	0	0	1/2	5.5(3)
N	0.04(2)	$-x$	$-0.01(6)$	8(5)
O	0.164(10)	0.233(5)	$-0.023(2)$	4.7(9)

with several initial models, in which two different NO$_2^-$ orientations were mixed with an equal probability (0.5), were unsuccessful.

3.3. Structure of phase II

According to the single-crystal x-ray diffraction study [2], phase II has a rhombohedral structure (space group: $R\bar{3}m$) in which the orientations of the NO$_2^-$ ions are disordered about a $\bar{3}$ axis. The following two models given by Solbakk and Strømme [2] were tested in the Rietveld analysis of the present neutron diffraction data. In model 1, the N atom is located on the $\bar{3}$ axis (at the 3a position), and the O atoms are located on a mirror plane (at the 18h position). In model 2, the N atom is placed on the mirror plane (at the 18h position), and the O atoms are placed at general positions (36i). Solbakk and Strømme favoured model 2 on the basis of the N–O bond lengths. For both models, Rietveld refinements were performed with the O–N–O bond angle fixed at 115°; the refinements did not converge without this constraint. Isotropic atomic displacement parameters were used for the final model because no significant improvement of the R_{wp}-value was achieved by using anisotropic ones. The R_{wp}-values obtained for models 1 and 2 were 4.01% and 3.88%, respectively. The N–O bond length in model 1 (1.00(2) Å) was much shorter than the literature value of 1.24 Å [10], while that for model 2 (1.18(4) Å) agreed well with it. These results strongly support model 2, in agreement with the x-ray diffraction study. The results of the Rietveld analysis with model 2 are illustrated in figure 8, and the refined structural parameters are listed in table 3. The structure of phase II has no relation to that of phase III. The space group and
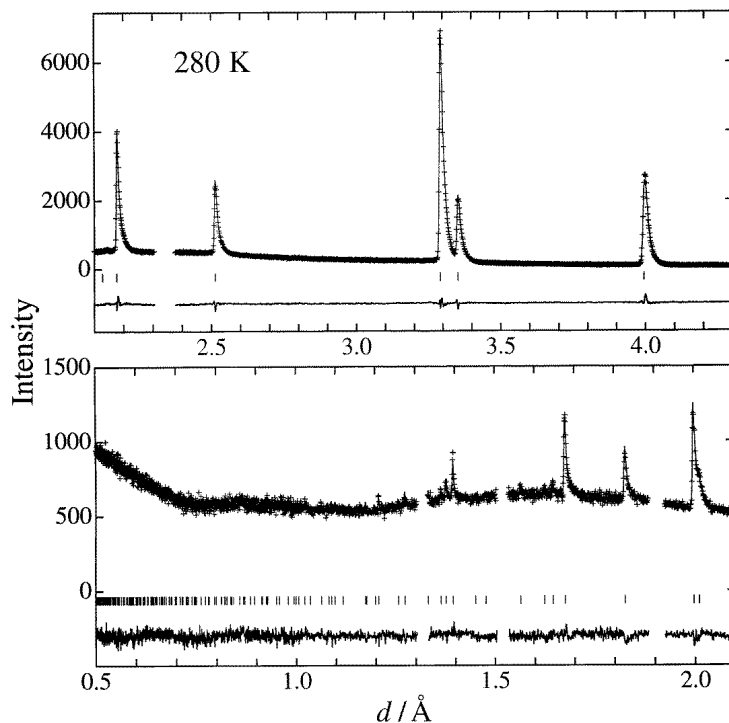
Figure 8. Observed (plus signs) and calculated (line) powder diffraction profiles of phase II at 280 K.

relative ionic positions of phase II are the same as those of KNO_3 phase I. In KNO_3 phase I, the NO_3^- ions have twofold orientational disorder, to satisfy the $\bar{3}m$ symmetry.

In this structural model of phase II, NO_2^- ions undergo sixfold orientational disordering. If one takes the large displacement parameters into consideration, the space distribution of the O atoms is almost continuous around the $\bar{3}$ axis, like a ring doughnut. This situation is reflected in the weak peak intensities in a lower-d-spacing region as shown in figure 8. The present result is also consistent with the large total excess entropy of the III–II transition $(25.9 \text{ J K}^{-1} \text{ mol}^{-1})$.

4. Conclusions

The neutron powder diffraction data of KNO_2 were collected at several temperatures at which phases III and II are stable, and the structures of these phases were successfully analysed by the Rietveld method. The structure of phase III is completely ordered at 4 K, and becomes gradually disordered as regards the orientation of the NO_2^- ions as the temperature increases toward the III–II transition temperature. In phase II, the orientations of the NO_2^- ions are highly disordered about the rhombohedral $\bar{3}$ axis. The present results are completely consistent with the previous calorimetric, NMR, and dielectric data, providing conclusive evidence for the orientational order/disorder of the NO_2^- ions in phases III and II of KNO_2.

References

[1] Mraw S C, Boak R J and Staveley L A K 1978 *J. Chem. Thermodyn.* **10** 359
[2] Solbakk J K and Strømme K O 1969 *Acta Chem. Scand.* **23** 300
[3] Kenmotsu M, Honda H, Ohki H, Ikeda R, Erata T, Tasaki A and Furukawa Y 1994 *Z. Naturf.* a **49** 247
[4] Honda H, Onoda-Yamamuro N, Ishimaru S, Ikeda R, Yamamuro O and Matsuo T 1998 *Ber. Bunsenges. Phys. Chem.* **102** at press
[5] Kamiyama T, Oikawa K, Tsuchiya N, Osawa M, Asano H, Watanabe N, Furusaka M, Satoh S, Fujikawa I, Ishigaki T and Izumi F 1995 *Physica* B **213+214** 875
[6] Boultif A and Loüer D 1991 *J. Appl. Crystallogr.* **24** 987
[7] Wolff P M 1968 *J. Appl. Crystallogr.* **1** 108
[8] Smith G S and Snyder R L 1979 *J. Appl. Crystallogr.* **12** 60
[9] Pawley G S 1981 *J. Appl. Crystallogr.* **14** 357
[10] David W I F, Ibberson R M and Matthewman J C 1992 *Rutherford Appleton Laboratory Report* RAL-92-032
[11] Ohta T, Izumi F, Oikawa K and Kamiyama T 1997 *Physica* B **234–236** 1093
[12] Kay M I, Frazer B C and Ueda R 1962 *Acta Crystallogr.* **15** 506
[13] Beevers C A and Trotman-Dickenson A F 1957 *Acta Crystallogr.* **10** 34
[14] Nimmo J K and Lucas B W 1973 *J. Phys. C: Solid State Phys.* **6** 201
[15] Sawada S, Nomura S and Fujii S 1958 *J. Phys. Soc. Japan* **13** 1549
[16] Moriya K, Matsuo T and Suga H 1983 *J. Phys. Chem. Solids* **44** 1121
[17] Moriya K, Matsuo T and Suga H 1983 *J. Phys. Chem. Solids* **44** 1103
[18] Moriya K, Matsuo T and Suga H 1988 *Bull. Chem. Soc. Japan* **61** 1911
[19] Honda H, Kenmotsu M, Ohki H, Ikeda R and Furukawa Y 1995 *Ber. Bunsenges. Phys. Chem.* **99** 1009
[20] Honda H, Ishimaru S, Onoda-Yamamuro N and Ikeda R 1995 *Z. Naturf.* a **50** 871
[21] Honda H, Kenmotsu M, Onoda-Yamamuro N, Ohki H, Ishimaru S, Ikeda R and Furukawa Y 1996 *Z. Naturf.* a **51** 761